

Path Loss Prediction Using Machine Learning with Extended Features

Jonathan Ethier, Mathieu Châteauevert, Ryan G. Dempsey, and Alexis Bose
Communications Research Centre Canada (CRC), Ottawa, Ontario, Canada
{jonathan.ethier, mathieu.chateauevert, ryan.dempsey, alexis.bose}@ised-isde.gc.ca

Abstract—Wireless communications rely on path loss modeling, which is most effective when it includes the physical details of the propagation environment. Acquiring this data has historically been challenging, but geographic information system data is becoming increasingly available with higher resolution and accuracy. Access to such details enables propagation models to more accurately predict coverage and minimize interference in wireless deployments. Machine learning-based modeling can significantly support this effort, with feature-based approaches allowing for accurate, efficient, and scalable propagation modeling. Building on previous work, we introduce an extended set of features that improves prediction accuracy while, most importantly, maintaining model generalization across a broad range of environments.

I. INTRODUCTION

In the modern age, propagation modeling has emerged as a cornerstone for enhancing communication networks and wireless technologies. With the proliferation of IoT devices [1], Fifth-Generation (5G) networks [2], and the advent of Sixth-Generation (6G) [3], accurate propagation models are vital. These models facilitate the prediction of radio wave behaviour in diverse environments, ensuring optimal performance, minimal interference, and efficient spectrum usage. As seamless connectivity becomes the standard, fast, accurate and scalable propagation models will become the norm.

Prior work [4] considered a highly constrained set of features (frequency, distance and total obstruction depth) to make accurate path loss predictions. This paper doubles the number of features used previously thereby improving model accuracy while not sacrificing the generalized behaviour of the model. Additional blind test sets are introduced to further confirm the richer feature set does not lead to overfitting, which can be a concern in feature-rich models [5].

This work can be considered as semi-path-specific modeling, blending empirical (statistical) and path-specific approaches. The use of the prefix “semi” is supported by the fact that many unique path profiles can have identical Geographic Information System (GIS) scalar features. Examples of path-specific modeling include the industry standard International Telecommunication Union Radiocommunication (ITU-R) P.1812-7 [6], as well as machine learning (ML)-based modeling approaches found in [7] and [8].

This work is related, though distinct from [7], where the goal in that paper was to construct path-specific path loss models, using the entire path profile as an input to the path loss model. The authors in [9] consider a small number of inputs to their model, though the features did not have a direct connection to physical GIS features. In [8], the authors develop

feature-rich, region-specific models that utilize random cross-validation as the method of assessing model performance, which does not assess model generalization [10] - a limitation we aim to address here.

In Section II we discuss the model and features, followed by a discussion of results in Section III, ending with our concluding remarks in Section IV.

II. PROPOSED METHOD

A. Data and Preprocessing

The training data used in this work is radio frequency (RF) drive test data [11] collected by the UK’s Office of Communications (Ofcom). This dataset contains measured path loss and the locations and heights of the transmitter and receiver. From the location and height information, path profiles can be extracted from UK Open Data [12], using supporting code from [13]. The Digital Terrain Model (DTM) and Digital Surface Model (DSM) are extracted from the GIS data. All subsequent features are derived from these sources of information. We only use samples above the measurement noise floor with an additional 6 dB margin. A total of 30 000 random samples meeting this noise criterion were extracted for each of the six measurement frequencies (449, 915, 1802, 2695, 3602, and 5850 MHz) within each of the six drive tests (London, Merthyr Tydfil, Nottingham, Southampton, Stevenage, Boston), resulting in a training set size of 1.08 million samples.

Additional proprietary drive test data was acquired from Netscout Systems Inc. [14], consisting of measurements from a variety of environments across Canada including dense urban, suburban, and rural regions. Ten regions were included, with over 120 000 measurements in total, spanning frequencies from 700 to 3700 MHz. Path profiles and their features were all acquired in the same manner as the UK drive tests, only using the High-Resolution Digital Elevation Model (HRDEM) [15] for the GIS information (DTM and DSM) because of the Canadian geographic locations. In all cases, Earth curvature is accounted for when extracting the DTM and DSM path profiles, using the mean radius of 6 731 km.

B. Model Features

Note that the features under consideration are all scalar quantities and are mostly derived from the intersection of the direct path (the line connecting the transmitter to the receiver) and DSM. Fig. 1 shows the extraction of all six features from a representative link, and Table I lists the six features.

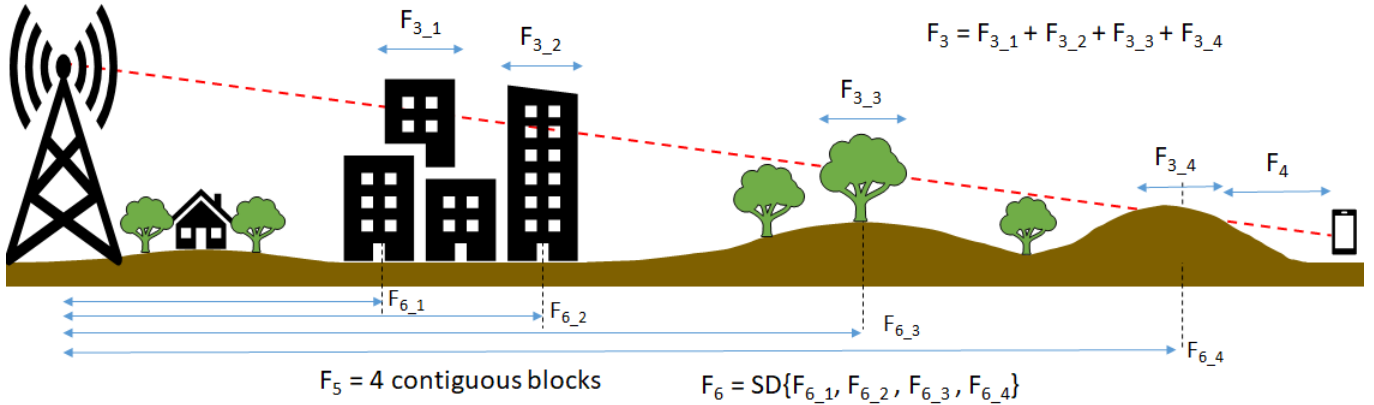


Fig. 1. Example path profile consisting of a mixture of buildings (black), terrain (brown) and foliage (green) obstructions with the direct path between transmitter and receiver shown in red. Since the model is agnostic to the type of blockage and uses DSM-only to assess obstructions, all obstructions are treated identically, and only their depths, count and locations matter when computing the six model features.

1) *Fundamental Features*: The two fundamental features present in nearly every propagation model are F_1 frequency and F_2 link distance (distance from the transmitter to the receiver). This allows the ML to model the path loss exponent and improve upon basic free space path loss.

2) *Obstruction Depth and Distance Features*: The next two features we introduce are F_3 total obstruction depth and F_4 distance from last obstruction to receiver. These features provide the model with the amount the direct path is obstructed from transmitter to receiver, as well as the amount of clear path there is from obstacles to receiver. When combined with link distance, several other distance metrics can be implicitly derived in model training.

3) *Obstruction Density and Distribution Features*: The next two features introduced are F_5 Contiguous Block Count and F_6 SD of Contiguous Block Locations. A contiguous block is defined as a contiguous obstruction along the direct path, with no blockage before and after the so-called block. We represent the total number of these blocks along the link with F_5 and the standard deviation (SD) of the distances from the transmitter to the center of the blocks with F_6 . Combining these two features with the total obstruction depth, F_3 , additional density metrics can be implicitly derived by the model during training.

TABLE I
FEATURE DESCRIPTIONS

Symbol	Feature
F_1	Frequency
F_2	Distance from Transmitter to Receiver
F_3	Total Obstruction Depth
F_4	Distance from Obstructions to Receiver
F_5	Contiguous Block Count
F_6	SD of Contiguous Block Locations

C. Model Architecture

Given the tabular nature of the features, dense neural networks are an appropriate model architecture [16] for modeling. The number of hidden layers and the number of units per

layer were optimized based on validation scores with the ideal structure of three hidden layers and 512 units per layer, resulting in at most 529 921 total parameters. A dropout layer was included after every hidden layer. Rectified linear unit (ReLU) activations were used to exploit non-linear interactions between features, except for the output layer which used a linear activation as is the default for regression tasks. We will assess the performance of three configurations of model inputs that follow a logical progression, as summarized in Table II, derived from Section II-B. The model architecture is shown in Fig. 2.

TABLE II
FEATURE CONFIGURATIONS, FEATURES FROM II-B

Configuration	Features
2 Features	F_1, F_2
4 Features	2 Features + F_3, F_4
6 Features	4 Features + F_5, F_6

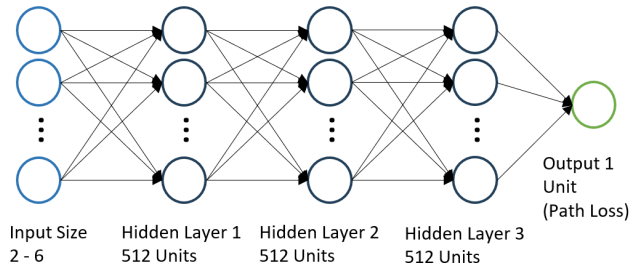


Fig. 2. Dense neural network architecture used in all models. Note that a dropout layer is included after each hidden layer, but only during training.

D. Training Approach

A round-robin train, validation, and test setup is used. Six holdout scenarios are constructed, each with one drive test held out of training, and the remaining five drive tests forming train

and validation. This provides six proper geographically (and morphologically) distinct test sets. Every test scenario is run 20 times independently, with random starting model coefficients and train/validation splits. The results of the 20 runs provide a mean and standard deviation (SD) of the root mean squared error (RMSE), allowing the performance and variation of the models to be judged.

Hyperparameters include: (a) random train and validation split of 80% / 20%, (b) batch size of 8192, (c) dropout of 25%, (d) Adaptive moment estimation (Adam) optimizer with an initial learning rate of 0.001 and (e) patience of 50 epochs. Mean squared error (MSE) is used as the loss function. The use of batch and layer norms were investigated but were shown to not improve validation scores and were therefore not used in the final architecture. All input features are normalized to have $\mu=0$ and $\sigma=1$, and only training samples are used to determine the normalization. Optimization runs require, on average, 90 epochs to converge, although this is largely a factor of our patience being set fairly high at 50 epochs.

III. RESULTS AND DISCUSSION

A. Model Performance, UK Blind Tests

A summary of the mean and SD RMSE test scores for the six drive test holdouts is shown in Table III. In nearly every holdout, the test RMSE decreases with the increasing number of features. The mean RMSE across the six holdouts decreases steadily to as low as 6.95 dB for six features. The Merthyr Tydfil holdout is the only test that bucks the trend, with the RMSE increasing slightly with six features. The Merthyr Tydfil drive test is largely characterized as hilly suburban, which is a land use type not present in the five drive test datasets used in training for that specific holdout. Consequently, the additional features do not yield lower prediction RMSE.

TABLE III
RMSE MEAN AND SD BY FEATURE COUNT, UK DRIVE TESTS

Holdout	2 Features		4 Features		6 Features	
	Mean	SD	Mean	SD	Mean	SD
London	11.57	0.32	7.29	0.14	6.62	0.06
Merthyr Tydfil	12.64	0.08	7.36	0.10	7.58	0.06
Nottingham	10.82	0.10	7.12	0.23	6.75	0.21
Southampton	10.88	0.21	7.09	0.18	6.42	0.18
Stevenage	10.17	0.09	8.28	0.08	7.20	0.08
Boston	12.83	0.29	7.35	0.50	7.13	0.53
Mean	11.48	0.18	7.42	0.20	6.95	0.19

B. Model Performance, Canadian Blind Tests

The results of the blind test holdouts shown in Section III-A provide strong evidence for model generalization. However, since the measurements were all performed in the same geographic region and by the same measurement team, there can still remain some lingering doubts regarding generalization. To address this potential concern, we investigate model performance on an additional set of blind tests introduced in Section II-A, the 10 drive tests conducted in Canada with over 120 000 samples in total.

We introduce a seventh model train/test scenario labeled as “No Holdout”. As the name implies, we use all six UK drive tests in train and validation, and test on the aggregate collection of Canadian drive tests. This provides the model with the full complement of UK drive tests, while conducting a blind assessment of the Canadian drive tests. There is no profound reason to have UK holdouts when blind testing on the Canadian drive tests, but the results are provided in Table IV nevertheless. A scatter plot of the predicted vs. measured test data for the generalized six-feature model is shown in Fig. 3 and the histogram of residuals is shown in Fig. 4. Note that the model with the lowest RMSE for all six holdouts, as well as “No Holdout”, is for the case of six features. An interesting outcome of these various blind tests is that the holdout models of Nottingham and Southampton have lower RMSE on the Canadian drive tests than the “o Holdout” model, despite the latter having greater variety and additional training samples. The Boston holdout has a notably higher test RMSE, indicating the importance of having the Boston drive test data in the training set. Lastly, the Merthyr Tydfil holdout does not suffer degraded performance on the Canadian data since hilly suburban drive tests were not present in the Canadian test data. These results strongly suggest that carefully curating the training data can provide advantages on test results, though one must be mindful of sequentially overfitting to the test data [17].

Since the six-feature model shows a consistently low mean RMSE, regardless of the train, validation and test configuration, we conclude that this is a well-generalized model. Additionally, given the low standard deviation of the mean RMSE, model selection is not highly sensitive, as most models are likely to exhibit consistently good performance.

The main takeaway from this section, and generally from this paper, is the performance of the “No Holdout” model, showing a mean blind test RMSE of 6.79 ± 0.14 dB, trained on all six UK drive tests, using the six features shown.

TABLE IV
RMSE MEAN AND SD BY FEATURE COUNT, CANADIAN DRIVE TESTS

Holdout	2 Features		4 Features		6 Features	
	Mean	SD	Mean	SD	Mean	SD
London	10.61	0.16	7.95	0.15	6.98	0.14
Merthyr Tydfil	10.98	0.14	7.92	0.18	6.91	0.12
Nottingham	10.33	0.15	7.21	0.17	6.62	0.11
Southampton	10.95	0.17	7.40	0.15	6.70	0.12
Stevenage	10.86	0.13	7.70	0.20	6.80	0.09
Boston	11.33	0.21	9.06	0.19	8.02	0.16
Mean	10.84	0.16	7.87	0.17	7.00	0.12
No Holdout	10.85	0.15	7.69	0.26	6.79	0.14

C. Deeper Dive into Model Selection

In Section III-A and Section III-B, we provided evidence for robust models since they all exhibit low variation of RMSE over 20 train/validation splits for progressively deeper blind testing scenarios. We can push this idea further by blindly

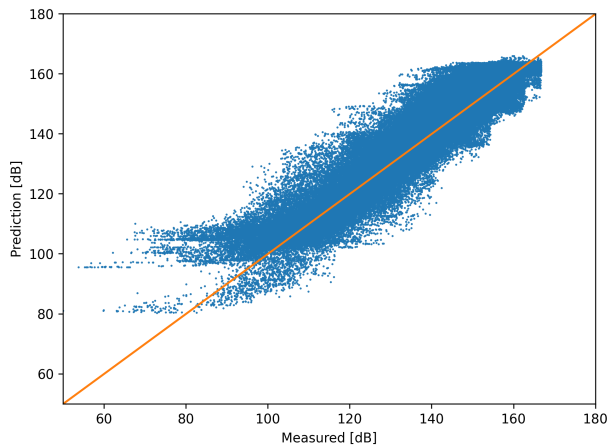


Fig. 3. Scatter plot of prediction vs. measured path loss, trained on all UK drive tests, blind test on Canadian drive tests. The orange line represents the line of perfect fit. This particular model has a coefficient of determination (denoted as R^2) equal to 0.88 and an RMSE of 6.96 dB.

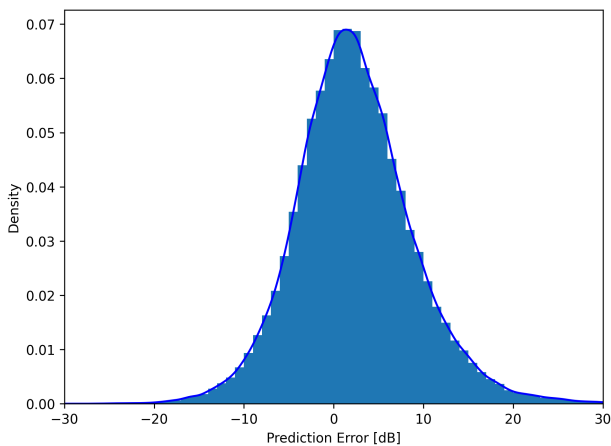


Fig. 4. Normalized histogram (with bounding envelope) of prediction residuals (same model as shown in Fig. 3). The mean and median error of this model is +2.33 and +1.98 dB, respectively.

trusting the validation score over larger optimization runs. We run the optimization of the six-feature model 200 times, with the resulting statistics summarized in Table V. If we specifically target the models with the lowest 20 validation scores from the 200 optimization runs, a mean test RMSE of 6.69 ± 0.13 dB is achieved. Though a modest improvement of 0.10 dB, the result shows that one can consistently achieve superior test scores by trusting the validation score in this training scenario.

IV. CONCLUDING REMARKS

This paper described the use of an extended set of scalar features to model path loss from 500 MHz to 6 GHz. An optimum set of six scalar features was identified, offering low prediction error in a generalized manner, achieving less than 7 dB RMSE on continentally distinct blind testing. Additional studies showed that the test performance does not suffer

TABLE V
RMSE STATISTICS FOR LONGER 200 OPTIMIZATION RUNS

RMSE	UK (Validation)	Canadian (Test)
Min	5.81	6.42
Max	6.07	7.12
Median	5.91	6.76
Mean (All 200 models)	5.91 ± 0.05	6.78 ± 0.13
Mean (Best 20 models)	5.83 ± 0.01	6.69 ± 0.13

from overfitting when over-relying on the validation scores. Despite the low prediction error, the model architecture is modest, and the feature extraction process from path profiles is straightforward, requiring only surface information.

Future work can involve extending the model to mmWave frequencies, incorporating additional features to better account for diffraction effects, and addressing the scenarios where the models are most inaccurate.

REFERENCES

- [1] A. Al-Fuqaha, M. Guizani, M. Mohammadi, M. Aledhari, and M. Ayyash, "Internet of things: A survey on enabling technologies, protocols, and applications," *IEEE Communications Surveys & Tutorials*, vol. 17, no. 4, pp. 2347–2376, 2015.
- [2] F. Boccardi, R. W. Heath, A. Lozano, T. L. Marzetta, and P. Popovski, "Five disruptive technology directions for 5g," *IEEE Communications Magazine*, vol. 52, no. 2, pp. 74–80, 2014.
- [3] W. Saad, M. Bennis, and M. Chen, "A vision of 6g wireless systems: Applications, trends, technologies, and open research problems," *IEEE Network*, vol. 34, no. 3, pp. 134–142, 2020.
- [4] J. Ethier and M. Châteauevert, "Machine learning-based path loss modeling with simplified features," *IEEE Antennas and Wireless Propagation Letters*, vol. 23, no. 11, pp. 3997–4001, 2024.
- [5] C. Bishop, *Pattern Recognition and Machine Learning*. Springer, 2006.
- [6] "P.1812: A path-specific propagation prediction method for point-to-area terrestrial services in the frequency range 30 MHz to 6000 MHz," International Telecommunications Union (ITU). [Online]: <https://www.itu.int/rec/R-REC-P.1812-6-202109-1/en>. Accessed December 2024.
- [7] R. G. Dempsey, J. Ethier, and H. Yanikomeroglu, "Path loss prediction using deep learning," 2024. [Online]. Available: <https://arxiv.org/abs/2411.17752>
- [8] T. Hayashi and K. Ichige, "A deep-learning method for path loss prediction using geospatial information and path profiles," *IEEE Transactions on Antennas and Propagation*, vol. 71, no. 9, pp. 7523–7537, 2023.
- [9] H.-S. Jo, C. Park, E. Lee, H. Choi, and J. Park, "Path loss prediction based on machine learning techniques: PCA, artificial neural network, and gaussian process," *Sensors*, vol. 20, p. 1927, 03 2020.
- [10] D.R. Roberts *et. al*, "Cross-validation strategies for data with temporal, spatial, hierarchical, or phylogenetic structure," *Ecography*, vol. 40, no. 8, pp. 913–929, 2017. [Online]. Available: <https://nsojournals.onlinelibrary.wiley.com/doi/abs/10.1111/ecog.02881>
- [11] Ofcom, "Open data." [Online]. Available: <https://www.ofcom.org.uk/about-ofcom/our-research/pendata>. Accessed December 2024.
- [12] "Open Data data.gov.uk," Government of the United Kingdom. [Online]. Available: <https://www.data.gov.uk/>. Accessed December 2024.
- [13] "Signal attenuation through foliage estimator (source code)," Communications Research Centre (CRC) Canada. [Online]. Available: <https://github.com/ic-crc/SAFE-Tool>. Accessed December 2024.
- [14] Path Loss Measurements using Continuous Wave Drive Tests in Canada (2020-2021). Netscout Systems Inc., 2022. [Online]. Available: <https://www.netscout.com/product/rf-modeling>
- [15] "High-Resolution Digital Elevation Model (HRDEM)," Natural Resources Canada (NRCan). [Online]. Available: <https://open.canada.ca/data/en/dataset/957782bf-847c-4644-a757-e383c0057995>. Dec. 2024.
- [16] I. Goodfellow, Y. Bengio, and A. Courville, *Deep Learning*. MIT, 2016.
- [17] M. A. Lones, "Avoiding common machine learning pitfalls," *Patterns*, vol. 5, no. 10, p. 101046, Oct. 2024. [Online]. Available: <http://dx.doi.org/10.1016/j.patter.2024.101046>